J Lipid Atheroscler. 2025 Sep;14(3):350-371
https://doi.org/10.12997/jla.2025.14.3.350
pISSN 2287-2892·eISSN 2288-2561

JLA Journal of Lipid and Atherosclerosis

Original Article

Check for updates

Exhaled Breath Biomarkers Reflect the Inflammasome and Lipidome Changes in Ischemic Heart Disease: A Study Using Machine Learning Models and Network Analysis

Basheer Abdullah Marzoog[1], **Peter Chomakhidze**[1], **Daria Gognieva**[1], **Artemiy Silantyev**[1], **Alexander Suvorov**[1], **Anastasia Stroeva**[1], **Malika Mustafina**[2], **Alina Yur'evna Fedorova**[3], **Abram Syrkin**[2], **Philipp Kopylov**[1]

[1]World-Class Research Center, Digital Biodesign and Personalized Healthcare, I.M. Sechenov First Moscow State Medical University (Sechenov University), Moscow, Russia
[2]Department of Cardiology, Functional and Ultrasound Diagnostics, I.M. Sechenov First Moscow State Medical University (Sechenov University), Moscow, Russia
[3]Interclinical Biochemical Department of the Central Laboratory and Diagnostic Service of Sechenov University, Moscow, Russia

OPEN ACCESS

Received: Feb 4, 2025
Revised: Apr 18, 2025
Accepted: May 13, 2025
Published online: Jul 8, 2025

Correspondence to
Basheer Abdullah Marzoog
World-Class Research Center, Digital Biodesign and Personalized Healthcare, I.M. Sechenov First Moscow State Medical University (Sechenov University), 8-2 Trubetskaya Street, Moscow 119991, Russia.
Email: marzug@mail.ru

ORCID iDs
Basheer Abdullah Marzoog
https://orcid.org/0000-0001-5507-2413
Peter Chomakhidze
https://orcid.org/0000-0003-1485-6072
Daria Gognieva
https://orcid.org/0000-0002-0451-2009
Artemiy Silantyev
https://orcid.org/0000-0001-8360-1415
Alexander Suvorov
https://orcid.org/0000-0002-2224-0019
Anastasia Stroeva
https://orcid.org/0009-0002-3694-5295
Malika Mustafina
https://orcid.org/0000-0002-0250-9949
Alina Yur'evna Fedorova
https://orcid.org/0000-0001-8283-5359

ABSTRACT

Objective: To define relationships between lipidomics, inflammasome, and exhaled volatile organic compounds (VOCs) in ischemic heart disease (IHD) and develop a VOC-based diagnostic machine learning model for non-invasive diagnosis.
Methods: A single-center prospective study involved 80 participants between 27 Oct 2023 and 11 Jun 2024: 31 with stress-computed tomography (CT) myocardial-perfusion–confirmed IHD and 49 perfusion-negative controls. All underwent stress CT perfusion, bicycle-ergometry, and breath collection at rest, peak exercise, and 3-minute recovery into a PTR-TOF-MS-1000. Lipid measurements were made (total, high-density lipoprotein [HDL]-, low-density lipoprotein [LDL]-, very LDL-cholesterol, triglycerides, apolipoprotein B [ApoB], lipoprotein-a) and inflammatory biomarkers (interleukin-6, C-reactive protein). LASSO regression mapped VOC–biomarker associations. An XGBoost classifier integrating VOCs, lipidome, inflammasome, and lipid-lowering therapy status was evaluated with cross-validated Youden index.
Results: Controls showed minimal biomarker-VOC relationships. Patients exhibited significant lipid-VOC correlations, including HDL-C with m/z 49.995 (r=0.31) and an inverse correlation between total cholesterol and m/z 94.053 (r=−0.35). Key discriminative VOCs were 2-ethyl-2,5-dihydro-4,5-dimethylthiazole, HO3PS2, CH8N3P, and m/z 49.995. Exercise revealed dynamic ApoB and LDL interactions exclusive to IHD. Inflammasome had limited direct VOC links; IL-6 inversely correlated with total cholesterol in IHD, while CRP aligned with HDL in controls. The final model achieved: AUC 0.931 (95% confidence interval [CI], 0.869–0.978), sensitivity 0.613 (95% CI, 0.435–0.793), specificity 1.000 (95% CI, 1.000–1.000), NPV 0.803 (95% CI, 0.692–0.903), PPV 1.000 (95% CI, 1.000–1.000).
Conclusion: Exhaled VOC patterns reflect lipid dysregulation in IHD. Combined with lipid and inflammatory data, VOCs enable high-accuracy, non-invasive IHD discrimination, supporting breathomics as a promising diagnostic adjunct.

JLA Journal of Lipid and Atherosclerosis

Abram Syrkin
https://orcid.org/0000-0002-9602-292X
Philipp Kopylov
https://orcid.org/0000-0001-5124-6383

Trial Registration
ClinicalTrials.gov Identifier: NCT06181799

Funding
The work of Philipp Kopylov was financed by the government assignment 1023022600020-6. Application of mass spectrometry and exhaled air emission spectrometry for cardiovascular risk stratification. The work of Philipp Kopylov was financed by RSF grant No. 24-15-00549. Development of methods for non-invasive diagnosis of chronic lung diseases using proton mass spectrometry of exhaled air and artificial intelligence methods.

Conflict of Interest
The authors have no conflicts of interest to declare.

Data Availability Statement
Will be provided upon reasonable request.

Author Contributions
Conceptualization: Marzoog BA, Kopylov P; Data curation: Marzoog BA, Chomakhidze P, Gognieva D, Fedorova AY, Syrkin A, Kopylov P; Formal analysis: Marzoog BA, Silantyev A, Suvorov A; Funding acquisition: Kopylov P; Investigation: Marzoog BA, Kopylov P; Methodology: Marzoog BA, Kopylov P; Project administration: Marzoog BA, Kopylov P; Resources: Marzoog BA, Kopylov P; Software: Marzoog BA, Suvorov A; Supervision: Kopylov P; Validation: Marzoog BA, Kopylov P; Visualization: Marzoog BA, Kopylov P; Writing - original draft: Marzoog BA, Gognieva D, Stroeva A, Mustafina M; Writing - review & editing: Marzoog BA, Kopylov P.

Trial Registration: ClinicalTrials.gov Identifier: NCT06181799

Keywords: Myocardial ischemia; Mass spectrometry; Inflammasomes; Lipidomics; CTP; Volatile organic compounds; Boosting machine learning algorithms

INTRODUCTION

Ischemic heart disease is increasingly recognized as a global health emergency, due to the dramatic rise in the number of affected individuals each year.[1] This increase is attributable in part to limitations in early diagnostic and preventive techniques. Current clinical guidelines recommend the use of non-invasive imaging, such as coronary computed tomography angiography (CCTA) with or without vasodilation testing, as the primary method for assessing ischemic heart disease (IHD), with selection determined by pre-test probability and local test availability.[2-6] However, CCTA is not available at all medical facilities, is expensive, and often requires patients to wait a week or more for the test.[7] Moreover, CCTA with vasodilation requires highly qualified professionals and the capability to manage complications, such as arrhythmias during intravenous administration of vasodilators such as adenosine triphosphate (ATP). As a result, physical stress tests—such as treadmill or bicycle ergometry—remain the primary means to determine the need for coronary angiography and to guide procedural decisions, including stenting.[7] Physical stress tests are easy to perform, cost-effective, widely available, and less time-consuming compared to CCTA. However, their diagnostic accuracy does not exceed 60%–70%.[4,8] Therefore, the development of a method that is simple, rapid, cost-effective, highly accurate, and available in both outpatient and inpatient settings is urgently needed. The use of exhaled breath analysis for IHD diagnosis represents a novel area within cardiology.

Several methods and techniques have been used to assess changes in the biochemical composition of exhaled breath, including selected electronic nose sensors and mass spectrometers operating in time-of-flight mode, some of which require pre-processing of the collected breath sample. Published studies have indicated that exhaled breath analysis may serve as a non-invasive “mirror” of cardiac health, including the detection of ischemia.[7,9-13]

The term "volatilome" refers broadly to the range of biochemical constituents in exhaled breath, commonly known as volatile organic compounds (VOCs). These VOCs are organic chemicals present in exhaled air as gaseous byproducts of metabolic processes, cellular activity, or interactions with exogenous sources such as environmental pollutants, diet, or the microbiota.[14] VOCs are characterized by high vapor pressure and low boiling points, which enable their presence in breath. As biomarkers, they provide real-time insights into biochemical and pathophysiological states, offering a promising non-invasive tool for understanding disease mechanisms, metabolic dysregulation, environmental exposures, and the development of novel diagnostics.[15]

Previous investigations have not comprehensively addressed changes in exhaled breath biomarkers associated with IHD. Furthermore, to date, there has been no study reporting on lipidome and inflammasome alterations in patients with IHD confirmed by stress computed tomography perfusion (CTP) imaging with vasodilation testing. Additionally, correlations between exhaled breath biomarkers, lipidome, and inflammasome markers in IHD patients have not yet been explored.

https://doi.org/10.12997/jla.2025.14.3.350

A recent study demonstrated elevated levels of acetone, ethanol, and phenol in the exhaled breath of patients with coronary artery disease.[16] However, this study was limited by unclear inclusion and exclusion criteria (not excluding patients with diabetes mellitus or chronic heart failure), a narrow VOC spectrum (only 36 VOCs measured), small sample size, use of offline analysis, and omission of bias assessment. A more recent study of 80 participants—including 31 patients with IHD confirmed by positive myocardial perfusion defect on stress CTP with ATP—discriminated IHD from non-IHD patients with a diagnostic accuracy (area under the curve [AUC]) of 84% using exhaled breath analysis with PTR-TOF-MS-1000.[17]

The current investigation is the first worldwide to report changes in exhaled breath in patients with IHD confirmed by CTP and to correlate these changes with the lipidome and inflammasome.

MATERIALS AND METHODS

1. Study design

This was a prospective, single-center, cross-sectional diagnostic study conducted in a case-control format. Two groups were included: the first group (n=31) comprised patients with a myocardial perfusion defect identified by stress CTP imaging with a vasodilation test using ATP. The second group (n=49) consisted of participants without a myocardial perfusion defect on CTP imaging with the vasodilation test using ATP (**Fig. 1**).

Exclusion and inclusion criteria are detailed in the **Supplementary Table 1**.

All participants provided written informed consent for participation and for anonymous publication of any related images. The study was approved by the local ethics committee of

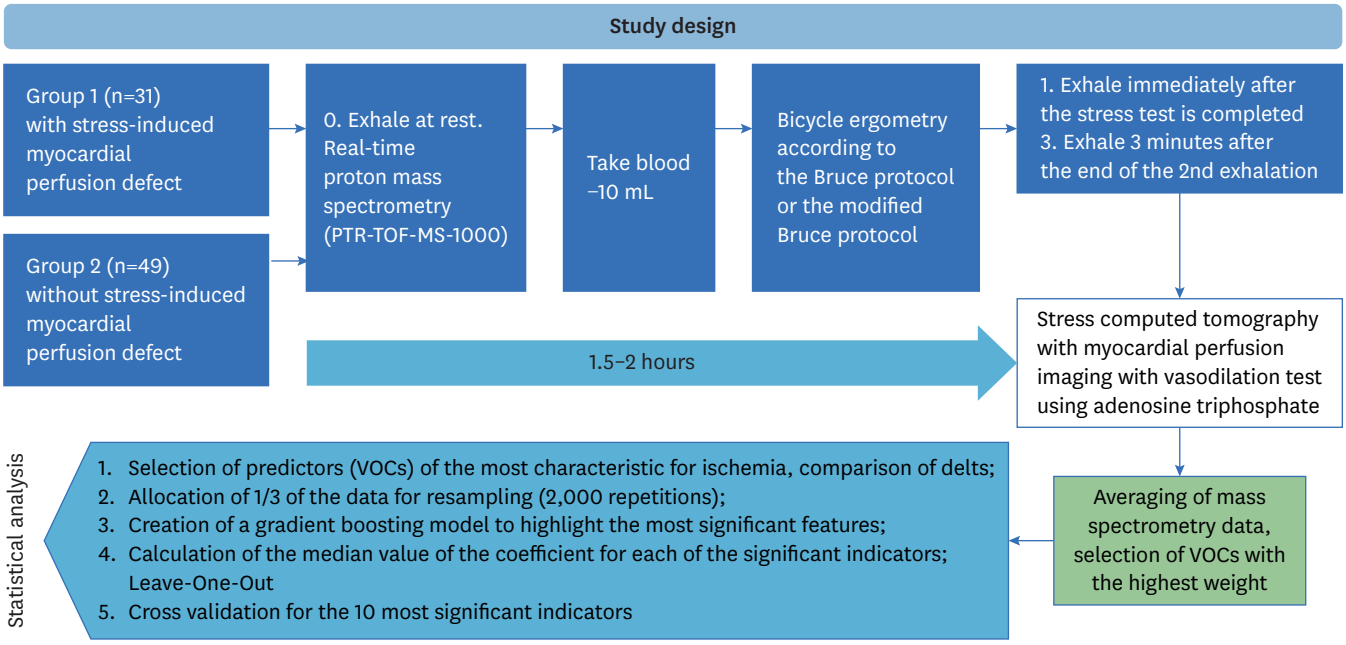

Fig. 1. Flow chart of the main study steps. The time spent at the hospital for the first 4 steps (blue background, white font) was 1.5–2 hours.
VOC, volatile organic compound.

https://doi.org/10.12997/jla.2025.14.3.350

Sechenov University (approval number 19-23, dated 26/10/2023). This study was conducted and reported in accordance with the STROBE guidelines.

2. Data collection

Data were collected at Hospital No. 1 of Sechenov University from October 27, 2023, to June 11, 2024. The study protocol was registered at ClinicalTrials.gov for full transparency (NCT06181799; https://clinicaltrials.gov/study/NCT06181799?a=1).

3. Instrumental analysis

All instrumental and laboratory analyses were performed in accordance with high-quality standards, following the Helsinki Declaration and Good Clinical Practice guidelines.

4. Stress CTP imaging with ATP

Before CTP imaging, all participants were required to provide recent (within 30 days) venous creatinine results and estimated glomerular filtration rate values per the 2021 chronic kidney disease-epidemiology collaboration creatinine formula (>30 mL/min/1.73 m^2), in accordance with recommendations from the National Kidney Foundation and the American Society of Nephrology.[18-21]

Both groups underwent venous catheterization via the basilic or radial vein for administration of contrast (Iohexol, Omnipaque) and Natrii (10 mg/1 mL; TRIPHOSADENINUM) to pharmacologically induce cardiac stress. The same catheter was used for contrast administration during CTP.

To prepare the ATP, 3 mL of ATP was diluted in 17 mL of isotonic sodium chloride solution (0.9%), resulting in a total of 20 mL per patient. The volume of diluted drug injected intravenously was calculated according to body weight: for 60 kg, 12 mL; for 70 kg, 14 mL; for 80 kg, 16 mL; and for 100 kg, 20 mL. Injection was performed manually over 2 minutes at a dose of 300 μg/kg.

Stress CTP imaging was performed using a Canon Aquilion One Genesis scanner (640 slices, 0.5 mm thickness) with intravenous administration of 50 mL of Iohexol contrast. The protocol consisted of 3 steps. First, a non-contrast scan was obtained to assess calcification in the cardiac valves and ascending aorta. Second, contrast was injected, and a rest-phase myocardial perfusion image was acquired. The patient then remained supine on the scanner for 20 minutes, after which ATP (10 mg/1 mL) was administered intravenously via catheter at a dose calculated according to body weight to induce pharmacological cardiac stress over 2 minutes. Immediately following the ATP stress test—within 30 seconds—a post-stress myocardial perfusion image was acquired.

5. Mass spectrometry (PTR-TOF-MS-1000)

At baseline, all participants underwent real-time mass spectrometry analysis of exhaled breath using the PTR-TOF-MS-1000 (IONICON PTR-TOF-1000-MS, Innsbruck). Testing was conducted in the hospital in the morning, with participants fasting and abstaining from exercise, food, and beverages (except water) for 6–8 hours beforehand.[22] Disposable sterile mouthpieces were used, and per manufacturer instructions, no additional filters were required. Participants exhaled into the sampler for 1 minute (12–16 exhalation cycles analyzed per participant). Ionized molecules were separated by mass-to-charge ratio (m/z) and detected. Mass spectra were acquired over an m/z range of 10–685 with a scan time of

1,000 ms and H_3O^+ as the primary ion. The T-Drift and T-Inlet temperatures were set at 80°C. The exhalation room was free of pollutants such as smoke or extraneous VOCs. To minimize external influences, participants used either public or personal transportation and avoided physical activity prior to testing.

Immediately after the bicycle ergometry, participants provided a second exhaled breath sample into the PTR-TOF-MS-1000 (1 minute). A third breath sample was collected 3 minutes after the second exhalation, also over 1 minute.

6. Physical exertion test

Participants first provided a baseline breath sample at rest using the PTR-TOF-MS-1000 real-time mass spectrometry device, in a controlled hospital environment with minimal atmospheric pollution. Following this, they underwent a bicycle ergometry test on a SCHILLER CS200 device, following either the Bruce protocol or a modified Bruce protocol to assess physiological responses to physical exertion. Immediately after completing the exercise test (within 1 minute), a second breath sample was collected using the same mass spectrometer. A third breath sample was obtained 3 minutes after the second exhalation, also within a 1-minute window.

Functional classification (FC) of angina for participants with positive stress test results was determined using metabolic equivalent of task (Mets-BT or BT) thresholds: BT/Mets values below 50/4 corresponded to FC-III, values between 50–100/4–7 indicated FC-II, and values exceeding 100/7 were classified as FC-I. Throughout the test, participants were continuously monitored using a 12-lead electrocardiogram (ECG), with manual blood pressure measurements recorded every 2 minutes, especially toward the end of each exercise stage.

The ergometry test was discontinued under the following conditions: systolic blood pressure ≥220 mmHg; horizontal or downsloping ST segment depression ≥1 mm on ECG; onset of angina-like chest pain; ventricular tachycardia; atrial fibrillation; or other clinically significant arrhythmias. The test was also terminated if the participant reached their target heart rate, defined as ≥86% of the age-predicted maximum (220 minus age).

7. Blood analysis

On the study day, all participants underwent a single venous blood draw in the morning (after bicycle ergometry, vascular stiffness testing, single-channel ECG, and exhaled air analysis, but before or after myocardial perfusion assessment as applicable). Ten milliliters of venous blood were collected in a biochemical test tube. The sample was centrifuged at 2,000 rpm for 20 minutes, and the resulting plasma was aliquoted into 7 Eppendorf tubes using sterile pipettes. Each tube was labeled with the participant's full name, and all tubes were placed in a single bag labeled with the participant's name, date of birth, date of blood collection, and investigator's signature. Samples were stored in a specialized ultra-low temperature refrigerator (–82°C to –84°C) until all collections were completed. Frozen plasma samples were then sent to the laboratory for analysis of total cholesterol, low-density lipoprotein (LDL), very low-density lipoprotein (VLDL), high-density lipoprotein (HDL), triglyceride (TG), C-reactive protein (CRP), lipoprotein(a), apolipoprotein B (ApoB), and interleukin-6 (IL-6). Lipid profile analyses (including total cholesterol, LDL, VLDL, HDL, TG, ApoB, and lipoprotein(a)) were performed on a Beckman Coulter AU-5800 automated biochemical analyzer (Beckman Coulter Inc., Brea, CA, USA), using Vector Best reagents. CRP and IL-6 were measured on the same analyzer with highly sensitive SRB-ELISA-BEST (RU No. RZN

https://doi.org/10.12997/jla.2025.14.3.350

2016/3872) and IL-6-ELISA-BEST (RU No. RZN 2022/18690) enzyme-linked immunosorbent assay (ELISA) kits. ELISA was used to assess inflammasome markers (CRP and IL-6). To ensure accuracy, laboratory staff were provided with an Excel spreadsheet listing participant names and required tests, allowing immediate data entry and minimizing the risk of error.

Reference values used in the study were obtained directly from the laboratory that conducted the analysis.

8. CVD risk stratification

Cardiovascular risk stratification was performed using the SCORE2 and SCORE2-OP tools for healthy participants, and the SMART risk score for individuals with positive perfusion defects on CTP with stress testing. Reference values for SCORE2, SCORE2-OP, and SMART risk score were obtained from established sources.[23,24]

9. Statistical analysis

For quantitative parameters, the distribution was assessed using the Shapiro–Wilk test, and summary statistics included mean, standard deviation, median, interquartile range, and minimum and maximum values. For categorical and qualitative variables, both absolute and proportional values were determined.

Comparisons of normally distributed quantitative variables between groups were performed using the Welch *t*-test; non-normally distributed variables were compared with the Mann–Whitney *U*-test. Categorical and qualitative features were analyzed using the Pearson χ^2 test, or the Fisher exact test when appropriate.

Given the relatively small sample size and the large number of variables analyzed, traditional group comparisons were often underpowered. Therefore, machine learning algorithms were employed for subsequent analyses.

10. Selection of significant predictors of perfusion defects and evaluation of model quality

The analytical workflow consisted of several stages:

1) Identification of exhaled breath metabolites associated with the outcome, and assessment of the strength of these relationships.
2) Evaluation of the associations between plasma lipid spectrum, lipid-lowering therapy, inflammatory markers (CRP, IL-6), and the outcome.
3) Construction of associative models between plasma biochemical parameters and selected exhaled breath metabolites in each group (patients and controls).

11. Determination of outcome-associated exhaled air metabolites and cross-validation using machine learning models

In the study, breath samples for mass spectrometry were collected at 3 defined time points (**Fig. 2**):

- Baseline: the patient exhaled calmly before any exertion.
- After stress: the patient exhaled immediately after the stress test.
- Recovery: the patient exhaled after 3 minutes of recovery after the stress test.

The deltas were calculated as the difference between the corresponding endpoint and the starting point. Thus, the deltas reflect the relative change in the intensity of the mass spectra.

https://doi.org/10.12997/jla.2025.14.3.350

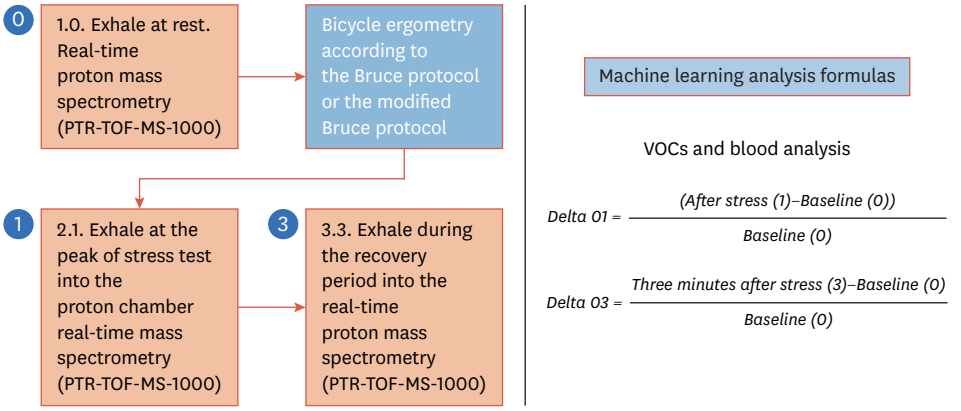

Fig. 2. Flowchart of machine learning analysis of exhaled breath. Numbers indicate time points: 0 = rest, 1 = peak exertion, 3 = 3 minutes after exertion.
VOC, volatile organic compound.

$$Delta\ 1 = \frac{After\ Stress\ (1) - Baseline(0)}{Baseline\ (0)}$$

$$Delta\ 3 = \frac{Three\ Minutes\ After\ Stress\ (3) - Baseline\ (0)}{Baseline\ (0)}$$

To identify relevant metabolites, we employed the XGBoost gradient boosting algorithm, which ranks predictors according to their importance.[25] The selection process was performed separately for 2 time intervals: the change in mass spectra immediately after completion of physical exertion (delta 1) and at the recovery time point (delta 3). To ensure robustness given the sample size, 2,000 iterations of resampling with replacement (full sample, n=80) were conducted. Data were normalized at each iteration using the RobustScaler from the scikit-learn v1.5.2 module. Predictor selection and feature importance ranking were repeated in each iteration using XGBoost. For each predictor, 2,000 importance values were obtained and summarized by the median. Predictors were then ranked in descending order of median importance. The top predictors with non-zero importance for both delta 1 and delta 3 intervals were selected, as well as those that were common to both time points ("common predictors").

For each interval and the set of common predictors, XGBoost models were built using repeated cross-validation (5 splits, 10 repeats). Model performance was evaluated using receiver operating characteristic (ROC) analysis, sensitivity, and specificity, with the optimal threshold determined by Youden's index.

12. Assessment of the relationships between plasma lipid spectrum indicators, the use of lipid-lowering therapy, and inflammatory markers with the outcome

A similar feature selection pipeline was applied to assess the associations between plasma biomarkers, lipid-lowering therapy, and the outcome. All plasma measurements (CRP, IL-6, total cholesterol and its fractions, ApoB, lipoprotein(a), and lipid-lowering therapy status) were performed at baseline, prior to exertion.

https://doi.org/10.12997/jla.2025.14.3.350

13. Associations between plasma biochemical parameters and selected metabolites in exhaled air

The study hypothesized that associations between plasma parameters, inflammatory markers, and exhaled air metabolites may differ between healthy participants and patients.

To robustly test this, 2,000 iterations of resampling with replacement were performed, and Spearman correlation coefficients between plasma variables and VOCs were calculated in each iteration. Correlation coefficients were then summarized by their median value across all iterations.

Associative network graphs were constructed, with edges included only if the median correlation coefficient exceeded 0.3 in absolute value. Only VOCs with significant associations to lipid spectrum or inflammatory markers were included.

This analysis pipeline was performed separately for both groups (patients and controls), for both time intervals (immediately after exertion and recovery), and for the set of common predictors. The goal was to identify VOCs whose changes were associated with lipid parameters or inflammation markers.

All statistical analyses were performed using R v4.2, Python v3.10, and Statistica 12 (StatSoft, Inc., 2014). Results were considered statistically significant at $p<0.05$.

RESULTS

A total of 101 individuals were initially enrolled, with 21 subsequently excluded due to discontinuation of participation. The final prospective cohort included 80 participants.

Based on CTP results, participants were divided into 2 groups: group 1 (n=31) with positive stress-induced myocardial perfusion defect, and group 2 (n=49) without stress-induced myocardial perfusion defect.

1. Descriptive statistics

Descriptive characteristics for the full sample and subgroups are provided in the tables. Continuous variables are detailed in **Table 1**.

Comparative characteristics for categorical variables are summarized in **Table 2**, stratified by presence or absence of post-stress induced myocardial perfusion defect on CTP with ATP.

2. The diagnostic accuracy of bicycle ergometry

The diagnostic performance of standard exercise testing on a bicycle ergometer was evaluated. ROC analysis using the physical exertion test result ("Reaction_type" = 'Positive') as the predictor and myocardial perfusion defect after stress ATP as the outcome yielded an AUC of 0.507 (95% confidence interval [CI], 0.388–0.625), sensitivity of 0.484 (95% CI, 0.306–0.657), specificity of 0.531 (95% CI, 0.392–0.673), negative predictive value of 0.619 (95% CI, 0.465–0.758), and positive predictive value of 0.395 (95% CI, 0.238–0.553).

https://doi.org/10.12997/jla.2025.14.3.350

Table 1. Descriptive statistics of the continuous variables of the full sample and groups

Variables	Full sample	Group 1	Group 2	*p*-value
Age (yr)	56.28 ± 10.60	59.93 ± 11.70	53.96 ± 9.23	0.013*
Pulse rate at rest (beats/min)	70.29 ± 9.55	70.22 ± 10.74	70.32 ± 8.84	0.960
SBP at rest (mmHg)	123.16 ± 15.43	124.48 ± 20.56	122.32 ± 11.22	0.545
DBP at rest (mmHg)	80.61 ± 11.23	82.35 ± 13.16	79.51 ± 9.81	0.270
Body weight (kg)	77.92 ± 16.23	77.12 ± 14.71	78.42 ± 17.25	0.730
Height (cm)	169.95 ± 8.83	169.80 ± 9.41	170.04 ± 8.54	0.900
BMI (kg/m^2)	26.93 ± 4.90	26.70 ± 4.23	27.06 ± 5.31	0.750
Goal heart rate (beat/min)	163.72 ± 10.60	160.06 ± 11.70	166.03 ± 9.23	0.013*
Maximum heart rate (beat/min)	146.25 ± 14.11	142.67 ± 17.66	148.51 ± 10.91	0.071
% from maximum heart rate	89.53 ± 9.16	89.42 ± 12.09	89.60 ± 6.84	0.930
WT	125.63 ± 44.11	120.96 ± 47.03	128.57 ± 42.38	0.450
METs	6.67 ± 1.97	6.32 ± 2.03	6.88 ± 1.92	0.220
Creatinine (μmol/L)	82.74 ± 16.01	80.37 ± 15.44	84.23 ± 16.34	0.290
eGFR (2021 CKD-EPI creatinine) mL/min/1.73 m^2	85.31 ± 14.68	84.85 ± 15.10	85.58 ± 14.53	0.820
Total cholesterol (mmol/L)	5.5 ± 1.47	5.61 ± 1.56	5.49 ± 1.43	0.710
TG (mmol/L)	1.3 ± 0.65	1.41 ± 0.77	1.16 ± 0.54	0.080
LDL (mmol/L)	3.4 ± 1.01	3.46 ± 1.08	3.27 ± 0.96	0.410
HDL (mmol/L)	1.4 ± 0.45	1.28 ± 0.34	1.44 ± 0.50	0.120
VLDL (mmol/L)	0.6 ± 0.29	0.64 ± 0.35	0.52 ± 0.25	0.080
Atherogenic index (calculated)	3.3 ± 1.42	3.60 ± 1.75	3.05 ± 1.14	0.090
ApoB (g/L)	1.1 ± 0.30	1.19 ± 0.35	1.08 ± 0.27	0.100
Lipoprotein a (mg/L)	238.0 ± 235.59	213.22 ± 207.23	253.67 ± 252.70	0.450
CRP (mg/L)	3.37 ± 3.19	3.81 ± 2.96	3.09 ± 3.33	0.330
IL-6 (pg/mL)	0.87 ± 1.04	0.88 ± 0.91	0.86 ± 1.12	0.950
SCORE2, SCORE2-OP	-	-	9.11 ± 6.99	
SMART risk score	-	15.07 ± 7.72	-	

Continuous sample variables are presented as mean ± standard deviation.
The Student *t*-test is used with independent variables.
SBP, systolic blood pressure; DBP, diastolic blood pressure; BMI, body mass index; WT, watt; MET, metabolic equivalent of task; eGFR, estimated glomerular filtration rate; CKD-EPI, chronic kidney disease-epidemiology collaboration; TG, triglyceride; LDL, low-density lipoprotein; HDL, high-density lipoprotein; VLDL, very low-density lipoprotein; ApoB, apolipoprotein B; CRP, C-reactive protein; IL-6, interleukin-6.
*Statistically significant difference values, $p<0.05$.

Table 2. Descriptive statistics of the categorical variables of the full sample and groups

Variables	Category	Full sample	Group 1	Group 2	*P*-value
Sex	Male	41 (51.25)	14 (45.16)	27 (55.10)	0.380
Weight and stage of obesity	Normal	30 (37.50)	12 (38.70)	18 (36.70)	0.980
	Overweight	29 (36.25)	11 (35.48)	18 (36.73)	
	Obesity (stage 1)	20 (25.00)	8 (25.80)	12 (24.48)	
	Obesity (stage 3)	1 (1.25)	0 (0.00)	1 (2.04)	
Smoking	No	66 (82.50)	24 (77.41)	42 (85.71)	0.340
Concomitant diseases	No	35 (43.75)	12 (38.70)	23 (46.93)	0.830
	Missing data	4 (5.00)	4 (12.90)	0 (0.00)	
Atherosclerosis of the coronary arteries	No	49 (61.25)	15 (48.38)	34 (69.38)	0.060
Hemodynamically significant atherosclerosis of the coronary arteries according to the results of computed tomography with assessment of myocardial perfusion (stenosis >70%)	No	71 (88.75)	23 (74.19)	48 (97.95)	0.002*
Stress-induced myocardial perfusion defect	No	49 (61.25)	0 (0.00)	49 (100.00)	<0.001*
Myocardial perfusion defect at rest	No	54 (67.50)	10 (32.25)	44 (89.79)	<0.001*
Atherosclerosis of arteries of other localizations	No	32 (40.00)	7 (22.58)	25 (51.02)	0.006*
	Missing data	7 (8.75)	2 (6.45)	5 (10.20)	
Arterial hypertension	No	40 (50.00)	12 (38.70)	28 (57.14)	0.100
Stage of arterial hypertension	I	5 (6.25)	4 (13.55)	1 (2.04)	0.070
	II	20 (25.00)	6 (19.35)	14 (28.57)	
	III	16 (20.00)	9 (29.03)	7 (14.28)	
Degree of arterial hypertension	1st degree	19 (23.75)	10 (32.25)	9 (18.36)	0.090
	2nd degree	13 (16.25)	3 (9.67)	10 (20.40)	
	3rd degree	9 (11.25)	6 (19.35)	3 (6.12)	

(continued to the next page)

https://doi.org/10.12997/jla.2025.14.3.350

Table 2. (Continued) Descriptive statistics of the categorical variables of the full sample and groups

Variables	Category	Full sample	Group 1	Group 2	*P*-value
History of IHD	Yes	3 (3.75)	4 (12.90)	1 (2.04)	<0.001*
	No	29 (36.25)	2 (6.45)	25 (51.02)	
	Missing data	48 (60.00)	25 (80.64)	23 (46.93)	
Type of blood pressure response to stress test	Asthenic	4 (5.00)	2 (10.50)	2 (4.08)	0.070
	Hypotonic	4 (5.00)	3 (15.80)	1 (2.04)	
	Hypertonic	8 (10.00)	1 (5.30)	4 (8.16)	
	Normotonic	64 (80.00)	1 (5.30)	0 (0.00)	
FC according to watts	FC I	8 (10.00)	1 (3.22)	7 (14.28)	0.310
	FC II	9 (11.25)	3 (9.67)	6 (12.24)	
	No IHD	63 (78.75)	27 (87.09)	36 (73.46)	
FC according to MET	FC I	6 (7.50)	1 (3.22)	5 (10.20)	0.550
	FC II	10 (12.50)	3 (9.67)	7 (14.28)	
	FC III	1 (1.25)	0 (0.00)	1 (2.04)	
	No IHD	63 (78.75)	27 (87.09)	36 (73.46)	
Type of stress test response	Negative	42 (52.50)	16 (51.61)	26 (53.06)	0.190
	Suspicious	21 (22.50)	11 (35.45)	10 (20.40)	
	Positive	17 (21.25)	4 (12.90)	13 (26.53)	
Reason for stopping the stress test	Horizontal ST >1 mm	8 (10.00)	2 (6.45)	6 (12.24)	0.380
	Reach target HR	72 (90.00)	29 (93.54)	42 (88.11)	
Exercise tolerance	Low	2 (2.50)	1 (3.22)	1 (2.04)	0.410
	Moderate	43 (53.75)	20 (64.45)	23 (46.93)	
	Close to high	8 (10.00)	3 (9.67)	5 (10.20)	
	High	16 (20.00)	3 (9.67)	13 (26.53)	
	Very high	11 (13.75)	4 (12.90)	7 (14.28)	
CKD stage	I	35 (43.75)	12 (38.70)	23 (46.93)	0.280
	II	41 (51.25)	16 (51.61)	25 (51.02)	
	IIIa	4 (5.00)	3 (9.67)	1 (2.04)	
Increase in TCH (mmol/L)	Normal	34 (42.50)	10 (32.25)	24 (48.97)	0.140
Increase in TG (mmol/L)	Normal	66 (82.50)	23 (74.19)	43 (87.75)	0.110
HDL reduction (mmol/L)	Normal	22 (27.50)	6 (19.35)	16 (32.65)	0.190
Increase LDL (mmol/L)	Normal	42 (52.50)	14 (45.16)	28 (57.14)	0.290
	High	38 (47.50)	17 (54.83)	21 (42.85)	
Increase in VLDL(mmol/L)	Normal	66 (82.50)	23 (74.19)	43 (87.75)	0.110
	High	14 (17.50)	8 (25.80)	6 (12.24)	
Atherogenic index (calc.)	Low	19 (23.75)	5 (16.12)	14 (28.57)	0.300
Increase in apolipoprotein B (g/L)	Normal	32 (40.00)	12 (38.70)	20 (40.81)	
	High	29 (36.25)	14 (45.16)	15 (30.61)	
Elevated lipoprotein (a) (mg/L)	Normal	61 (76.25)	21 (67.74)	40 (81.63)	0.150
Elevated IL-6 (pg/mL)	Normal	59 (73.75)	24 (77.41)	35 (71.42)	0.550
Elevated CRP (mg/L)	Normal	80 (100.00)	31 (100.00)	49 (100.00)	1.000
Hypolipidemic therapy	Normal	61 (76.25)	20 (64.51)	41 (83.67)	0.040*
Elevated VLDL (mmol/L)	Yes	15 (18.75)	6 (19.35)	9 (14.75)	0.910
	No	65 (81.25)	25 (80.64)	40 (65.57)	
SCORE2/SCORE2-OP	Low	-	-	10 (20.40)	
	Moderate	-	-	21 (42.85)	
	High	-	-	18 (36.73)	
SMART risk score	Low	-	11 (35.48)	-	
	Moderate	-	15 (48.38)	-	
	High	-	5 (16.12)	-	

Values are presented as number (%).
IHD, ischemic heart disease; FC, functional class; MET, metabolic equivalent of task; HR, heart rate; CKD, chronic kidney disease; TCH, total cholesterol; TG, triglyceride; HDL, high-density lipoprotein; LDL, low-density lipoprotein; VLDL, very low-density lipoprotein; IL-6, interleukin-6; CRP, C-reactive protein.
*Statistically significant difference values, $p<0.05$.

3. Lipidome and inflammasome changes with breathome changes

The lipid profile and inflammasome results were analyzed across 3 time points to optimize predictor selection and increase confidence in findings. The following steps were performed:

https://doi.org/10.12997/jla.2025.14.3.350

Step 1: selection of significant predictors of perfusion defects and evaluation of model quality
Following feature selection procedures for the interval between baseline and completion of exercise, the most outcome-associated predictors were identified based on 2,000 iterations, using their median feature importance within the model. The key VOCs identified at the baseline stage included: 144.91780 (0.00938), 159.07365 (0.00803), 56.053529 (0.00718), 59.057819 (0.00385), 72.053678 (0.00223), 355.06911 (0.00217), 71.054029 (0.00212), 49.995012 (0.00195), 43.047418 (0.00184), 148.046732 (0.00171), 94.0537307 (0.00159), 44.9914437 (0.00138), 447.104551 (0.00137), 63.0213147 (0.00095), 144.084727 (0.00094), 359.066780 (0.00084), 430.085362 (0.00062), and 175.134685 (0.00043).

The model rebuilt with these features demonstrated high predictive quality, with an AUC of 0.968 (95% CI, 0.931–0.993), sensitivity of 0.903 (95% CI, 0.786–1.000), specificity of 0.918 (95% CI, 0.833–0.981), negative predictive value of 0.938 (95% CI, 0.857–1.00), and positive predictive value of 0.875 (95% CI, 0.75–0.931).

During the recovery phase, a different set of VOCs showed the strongest association with the outcome. Those most important during recovery included: 51.03878 (0.01694), 49.99501 (0.01478), 132.05190 (0.01418), 144.91780 (0.01034), 87.076848 (0.00865), 94.053730 (0.00587), 87.933677 (0.0047), 118.07092 (0.00376), 110.05349 (0.00205), 144.08472 (0.00158), 44.014505 (0.00153), 297.08451 (0.00121), and 119.95504 (0.00009).

The rebuilt model for the recovery period also demonstrated strong performance, with an AUC of 0.994 (95% CI, 0.981–1.000), sensitivity of 0.903 (95% CI, 0.788–1.000), specificity of 0.980 (95% CI, 0.935–1.000), negative predictive value of 0.941 (95% CI, 0.873–1.000), and positive predictive value of 0.966 (95% CI, 0.889–1.000).

A subset of VOCs—144.08472, 144.91780, 49.995012, and 94.053730—were identified as common predictors for both time intervals. A model constructed using only these common VOCs demonstrated moderate predictive performance, with an AUC of 0.931 (95% CI, 0.869–0.978), sensitivity of 0.613 (95% CI, 0.435–0.793), specificity of 1.000 (95% CI, 1.000–1.000), negative predictive value of 0.803 (95% CI, 0.692–0.903), and positive predictive value of 1.000 (95% CI, 1.000–1.000). Complete tables with all predictors and values derived from the XGBoost analysis are available in **Supplementary Tables 2** and **3**.

Step 2: assessment of the relationships between plasma predictors and the outcome
When selecting plasma predictors, lipid-lowering therapy was included as a variable. The resulting predictors, ranked by feature importance, were: HDL (0.110409), lipid-lowering drugs (0.108628), CRP (0.107933), lipoprotein(a) (0.103706), IL-6 (0.103494), total cholesterol (0.10115), ApoB (0.0975365), TG (0.0893278), LDL (0.0754772), and VLDL (0.000).

It should be emphasized that the prominent role of lipid-lowering therapy reflects the higher likelihood of such therapy in patients with perfusion defects, which supports the validity of the boosting model's selection. To assess the independent contribution of biochemical parameters, lipid-lowering therapy was excluded from the model, resulting in a substantially reduced predictive quality, with an AUC of 0.528 (95% CI, 0.367–0.568), sensitivity of 0.290 (95% CI, 0.133–0.45), specificity of 0.653 (95% CI, 0.521–0.784), negative predictive value of 0.593 (95% CI, 0.463–0.717), and positive predictive value of 0.346 (95% CI, 0.161–0.52). The low performance likely reflects the weak relationship between single time-point plasma lipid

and inflammatory markers and outcomes from the exercise or recovery phases, as well as the limitation that plasma was sampled only prior to exertion.

Step 3: associations between plasma biochemistry and sampled VOCs
Correlation matrices and network graphs were generated after preprocessing and group stratification as described in the Methods.

In the visualizations, the thickness of each graph edge reflects the median correlation coefficient, while the color indicates direction (red for negative, blue for positive). The size of the nodes corresponds to their valence by module, where valence or order of a graph vertex is the number of edges for which this vertex is a node, taking into account the weight (i.e., correlation coefficient) of the edge.

The analysis confirmed that known associations, such as direct moderate correlations between inflammatory markers and strong correlations between lipid spectrum indicators, were present in both groups, mirroring the logic of the Friedewald formula.

Upon analyzing changes immediately after physical activity, spectral indicators such as total cholesterol, HDL, LDL, and ApoB were negatively associated with VOCs in the patient group, while positive associations were seen for lipoprotein(a). These patterns were not observed in the healthy group (**Fig. 3**, **Supplementary Tables 4** and **5**).

In the pre-recovery analysis, in the patient group, CRP and IL-6 were negatively associated with VOCs, and Lp(a) remained positive. In controls, total cholesterol and HDL were negatively associated with VOCs, and ApoB was positive (**Fig. 4**, **Supplementary Tables 6** and **7**).

When considering graphs based on common VOCs, in the main group, a moderate association is observed between these VOCs and HDL (positive correlation) as well as with total cholesterol (negative correlation). In the control group, a moderate positive association can be visualized between these VOCs and TG, VLDL, and ApoB (**Fig. 5**, **Supplementary Tables 8** and **9**).

4. Annotation of the obtained m/z (mass/charge)

The annotation was performed in several steps:

At the first stage, for each mass-charge ratio (m/z), all possible gross formulas were found based on the following hypothesis space:

1) We only considered [M+H] adducts;
2) The molecule could include the following elemental composition:
    1. C from 0 to 10;
    2. H from 0 to 50;
    3. N from 0 to 10;
    4. O from 0 to 10;
    5. P from 0 to 10;
    6. S from 0 to 10;
    7. The molecule should not include halogens (Cl, Br, I, or F);
    8. Rings and double bond equivalents (RDB) from −0.5 to 20;
    9. Error in determining the weight up to 50 ppm.

https://doi.org/10.12997/jla.2025.14.3.350

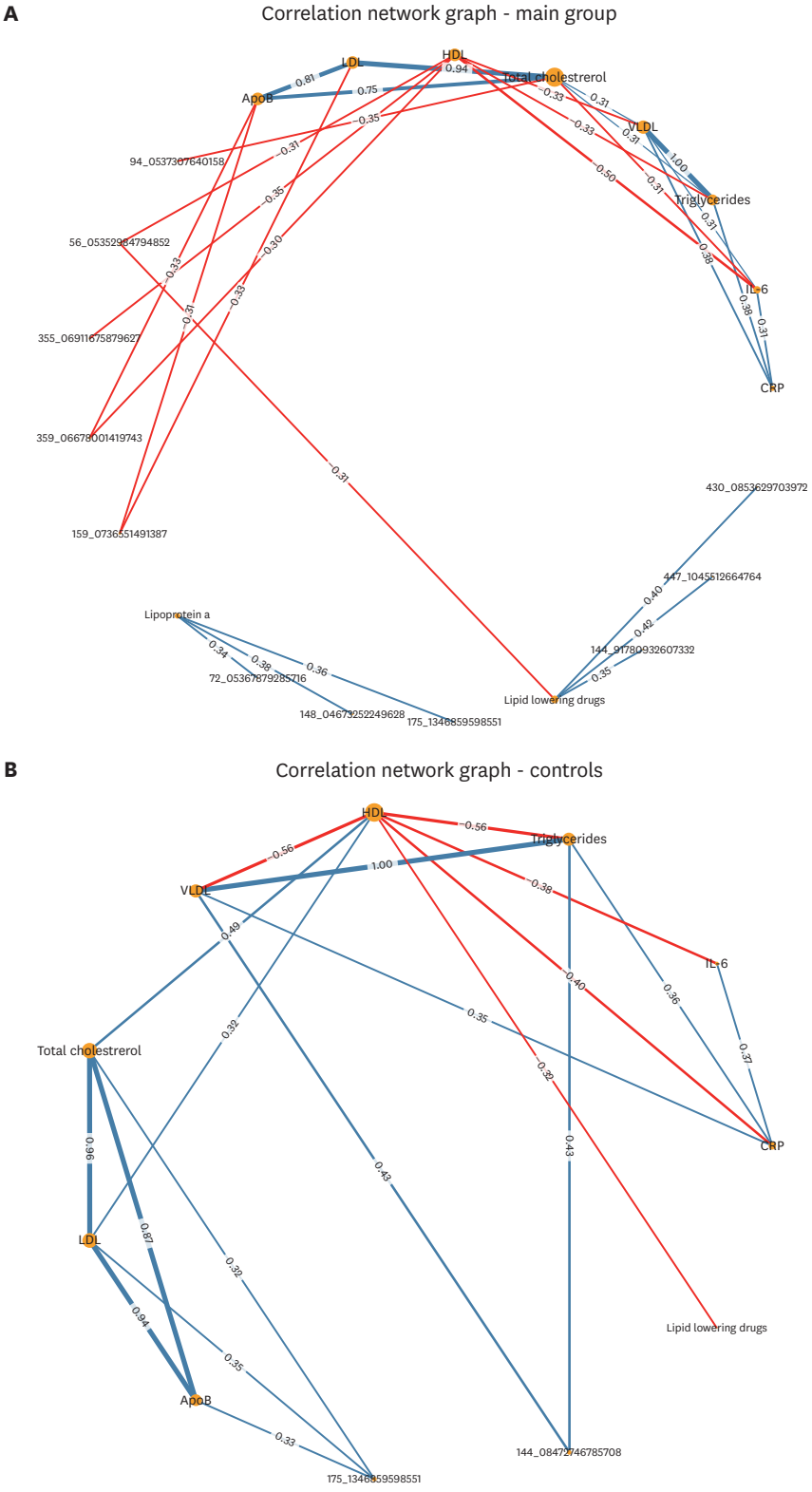

Fig. 3. Associations between ML-derived VOC signatures, lipid profile, and inflammation biomarkers in delta 1. (A, B) Correlations between key volatile organic compounds (identified via machine learning) and lipid profile, hypolipidemic therapy, and inflammatory markers (IL-6, CRP), spanning baseline to completion of exercise. Edge thickness reflects median correlation; color indicates direction (red: inverse, blue: direct). Correlations below 0.3 are omitted.
ML, machine learning; VOC, volatile organic compound; IL-6, interleukin-6; CRP, C-reactive protein; ApoB, apolipoprotein B; LDL, low-density lipoprotein; HDL, high-density lipoprotein; VLDL, very low-density lipoprotein.

https://doi.org/10.12997/jla.2025.14.3.350

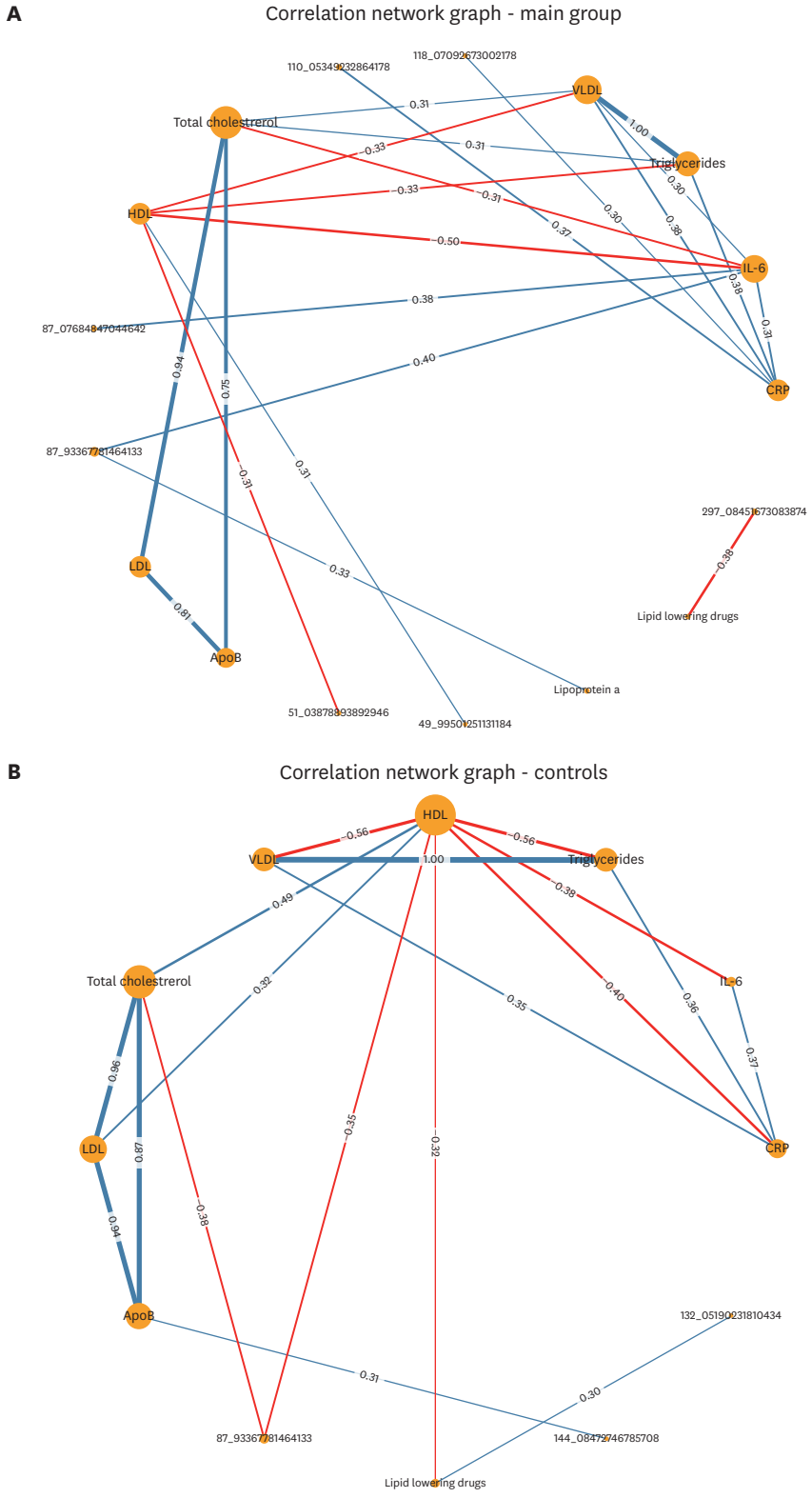

Fig. 4. Associations between ML-derived VOC signatures, lipidome, and inflammation biomarkers in delta 3. (A, B) Correlations of key volatile organic compound predictors, identified by the machine learning model, with lipid profile, use of hypolipidemic therapy, and inflammatory markers (IL-6 and CRP), spanning baseline to completion of exercise. Edge thickness reflects median correlation; color indicates direction (red: inverse, blue: direct). Correlations below 0.3 are omitted. ML, machine learning; VOC, volatile organic compound; IL-6, interleukin-6; CRP, C-reactive protein; VLDL, very low-density lipoprotein; HDL, high-density lipoprotein; LDL, low-density lipoprotein; ApoB, apolipoprotein B.

https://doi.org/10.12997/jla.2025.14.3.350

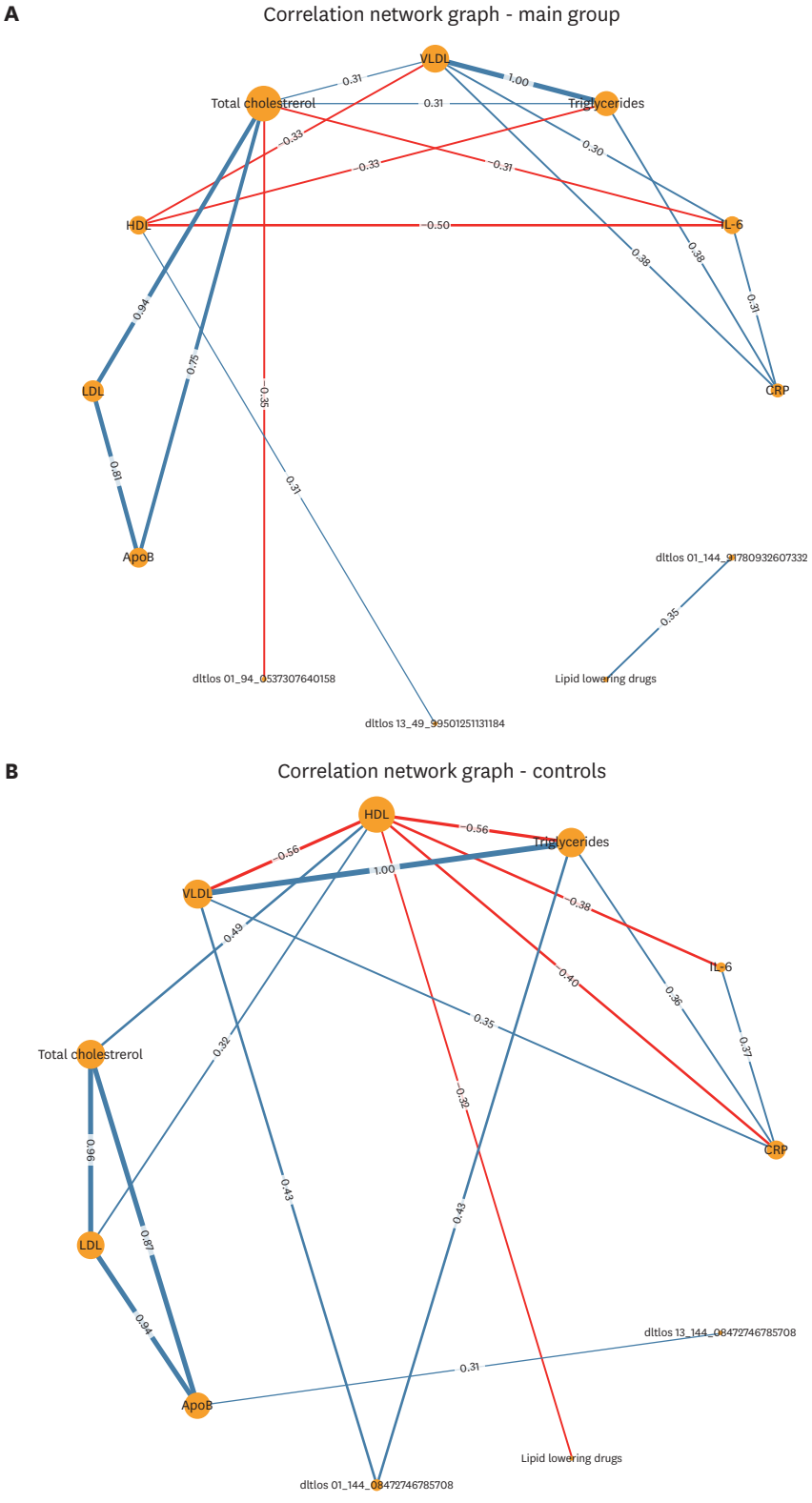

Fig. 5. Associations between common ML-derived VOC predictors, lipidome, and inflammation biomarkers for both delta 1 and delta 3. (A, B) Correlation of key volatile organic compound predictors (common to both time intervals) with lipid profile, use of hypolipidemic therapy, and inflammatory markers (IL-6 and CRP) in the main and control groups. Edge thickness reflects median correlation; color indicates direction (red: inverse, blue: direct). Correlations below 0.3 are omitted. ML, machine learning; VOC, volatile organic compound; IL-6, interleukin-6; CRP, C-reactive protein; VLDL, very low-density lipoprotein; HDL, high-density lipoprotein; LDL, low-density lipoprotein; ApoB, apolipoprotein B.

https://doi.org/10.12997/jla.2025.14.3.350

At the second stage, a match search was carried out in the Human Metabolome Database library for each resulting formula under the following conditions:

1) Exact molecular formula match;
2) The search was limited to m/z values below 200 due to the large number of possibilities above this threshold.

If no suitable gross formula could be found for a particular m/z, only the m/z value is reported. See **Table 3**[26] for a comparative presentation of the most significant VOCs, and consult the supplementary file (**Supplementary Table 10**) for the full list of possible chemical identities corresponding to the detected m/z values.

5. Limitations of this study

The primary limitation of this study is the modest sample size, which may introduce potential bias into the results. To mitigate this, we employed resampling techniques over a large number of iterations, robust data normalization, and median-based averaging (a more stringent approach than using the mean). Additionally, several findings in our study are consistent with established knowledge—such as the observed order of correlations in the lipid spectrum (in line with the Friedewald formula) and expected relationships between proinflammatory markers—which helps increase confidence in the validity of the results.

Another limitation concerns the proposed methodology itself: currently available spirograph devices are large and expensive, which limits their widespread use in clinical practice. For broader implementation, it will be necessary to develop compact, portable devices capable of detecting VOCs specific to ischemic heart disease—a process that will entail significant financial investment and development time. The lack of standardized protocols and incomplete reference libraries for ischemic heart disease-specific biomarkers also reduce the reproducibility and accuracy of this approach. Thus, clinical application will require unified protocols and expansion of these reference databases.

Finally, the small sample size in this study restricts the reliability and generalizability of our conclusions. Large-scale clinical trials with external validation are needed to confirm the effectiveness of this approach—combining exhaled breath biomarkers, inflammasome, and lipidome analysis—for the diagnosis of ischemic heart disease.

DISCUSSION

No statistically significant difference was found in the concentrations of lipidome biomarkers between the 2 groups. This finding is likely related to the presence of different types of ischemia detected by CTP—specifically, microvascular ischemia (ischemia with non-obstructive coronary artery disease [INOCA]) and atherosclerotic ischemia.[27] The pathophysiology underlying these forms of ischemia is distinct. In INOCA, microvascular vasospasm is the primary mechanism, leading to a mismatch between myocardial oxygen supply and demand. Such vasospasm is more often associated with inflammatory changes than with alterations in the lipidome. As a result, inflammasome biomarkers tended to be higher in the IHD group (group 1), where myocardial perfusion defects were frequently present without significant coronary artery stenosis. This supports the notion that inflammatory biomarkers may be more reliable indicators for both microvascular and macrovascular types of myocardial ischemia.[28]

https://doi.org/10.12997/jla.2025.14.3.350

JLA Journal of Lipid and Atherosclerosis

Table 3. Comparative listing of the most significant volatile organic compounds identified by exhaled breath analysis in individuals with and without ischemic heart disease

m/z in our study	Name of the chemical substance	Chemical formula	Annotation method	Mass error	Coeff	Error (ppm)	References
43.04741899	N/A	N/A	N/A	N/A	0.00184	N/A	[26]
44.01450529*	Cyanate	CHNO	HMD	−0.0014148530245989832	0.00153	−32.14515340515334	[26]
44.99144371	N/A	N/A	N/A	N/A	0.00138	N/A	[26]
49.99501251	N/A	N/A	N/A	N/A	0.00195	N/A	[26]
49.99501251	N/A	N/A	N/A	N/A	0.01478	N/A	[26]
51.03878894	N/A	N/A	N/A	N/A	0.01694	N/A	[26]
56.05352985	N/A	N/A	N/A	N/A	0.00718	N/A	[26]
59.05781995	Acetamidine	C2H6N2	HMD	0.0025544869753986177	0.00385	43.254000529672744	[26]
63.02131476*	N/A	C5H2	HMD	0.0016116769754006555	0.00095	25.573521935210344	[26]
71.05402914	N/A	N/A	N/A	N/A	0.00212	N/A	[26]
72.05367879*	Dihydrotriazole	C2H5N3	HMD	0.001944646975402975	0.00223	26.988864525163752	[26]
87.07684847*	N/A	C5H10O	HMD	0.0035929669754040106	0.00865	41.26202358646307	[26]
87.93367781	N/A	N/A	N/A	N/A	0.0047	N/A	[26]
94.05373076*	Methylphosphoramide	CH8N3P	HMD	−0.000870323024585673	0.00159	−9.253466263943373	[26]
94.05373076*	Methylphosphoramide	CH8N3P	HMD	−0.000870323024585673	0.00587	−9.253466263943373	[26]
110.0534923*	N/A	CH7N3O3 or C4H5N4	HMD	0.0025261369754048246 or 0.005205136975405367	0.00205	22.953719346940023 or 47.296427097619386	[26]
118.0709267*	Indole	C8H7N	HMD	−0.00580126302459405	0.00376	−49.13371298706043	[26]
119.9550439*	N/A	C2HNOS2	HMD	0.002188536975396005	0.00009	18.24464319499953	[26]
132.0519023*	N/A	C2H5N5O2	HMD	−0.0003008630245915356	0.01418	−2.2783694846593328	[26]
144.0847275*	2-Ethyl-2.5-dihydro-4.5-dimethylthiazole	C7H13NS	HMD	−0.0005810630245832726	0.00094	−4.032787059844858	[26]
144.0847275*	2-Ethyl-2,5-dihydro-4,5-dimethylthiazole	C7H13NS	HMD	−0.0005810630245832726	0.00158	−4.032787059844858	[26]
144.9178093	Phosphorothioic acid	HO3PS2	HMD	−5.8863024577249234e-05	0.00938	−0.40618213083386184	[26]
144.9178093	Phosphorothioic acid	HO3PS2	HMD	−5.8863024577249234e-05	0.01034	−0.40618213083386184	[26]
148.0467325*	1-Methyl-2-nitro-1-nitrosoguanidine	C2H5N5O3	HMD	−0.00021606302456689264	0.00171	−1.4594244730588204	[26]
159.0736551*	N/A	C6H10N2O3	HMD	0.0027643369754173364	0.00803	17.377717093880598	[26]
175.134686*	N/A	C12H16N	HMD	0.0008644369754335912	0.00043	4.93584106710644	[26]
297.0845167*	N/A	N/A	N/A	N/A	0.00121	N/A	N/A
355.0691168*	N/A	N/A	N/A	N/A	0.00217	N/A	N/A
359.06678*	N/A	N/A	N/A	N/A	0.00084	N/A	N/A
430.085363*	N/A	N/A	N/A	N/A	0.00062	N/A	N/A
447.1045513*	N/A	N/A	N/A	N/A	0.00137	N/A	N/A

Values shown in bold represent m/z ratios that were common to the baseline, immediately post-exercise, and recovery time intervals.
The m/z (mass-to-charge) ratios reported in our study closely correspond to values published in the literature or found in the Human Metabolome Database. Where an m/z ratio does not have a known chemical name, it is presented as a chemical formula.
N/A, not available.
*An asterisk indicates that the m/z may correspond to 2 or more different chemical substances.

https://doi.org/10.12997/jla.2025.14.3.350

By contrast, the pathophysiology of ischemia with obstructive coronary artery disease is classically driven by dyslipidemia. Accordingly, participants with this form of ischemia typically had elevated levels of atherogenic lipids such as LDL and TG. Notably, inflammatory biomarkers (CRP and IL-6) were also higher in IHD patients, reflecting the well-established link between inflammation and atherosclerosis. Many of these patients were also prescribed lipid-lowering agents such as statins.

Several interesting associations emerged between lipid spectra and inflammatory markers, though the inflammatory marker levels themselves were not directly or strongly correlated with VOCs. In contrast, multiple correlations were observed for the lipid spectrum, particularly in the patient group:

1) Immediately after the load:
   - In the main group:
     - ✓ Negative correlations with ApoB, HDL, LDL, and total cholesterol (TCH) in the study group
     - ✓ Positive correlations with LPA in the study group
     - ✓ Positive correlations with various VOCs in the study group among patients receiving lipid-lowering therapy
   - In the control group:
     - ✓ Significantly fewer correlations
     - ✓ Positive correlations between the lipid spectrum and VOCs
2) Three minutes after the second breath
   - In the main group:
     - ✓ Important positive correlations with IL-6 and substances with highly similar mass spectra
     - ✓ Positive correlations between 2 VOCs and CRP
     - ✓ Only HDL (multidirectional) and LPA had correlations with VOCs
     - ✓ There was a moderate negative relationship between the prescription of lipid-lowering therapy and some high-weight VOCs (i.e., VOC levels were higher in those who were not prescribed therapy).
   - In the control group:
     - ✓ Significantly fewer correlations
     - ✓ The correlations of TCH and HDL with VOCs were negative, with ApoB and lipid-lowering therapy having positive correlations.
3) Common VOCs at both points:
   - In the main group:
     - ✓ No common VOCs (at both time stages)
   - In the control group:
     - ✓ Significantly fewer correlations
     - ✓ Only 1 VOC was common to both periods, directly related to the lipid spectrum.

A key observation across all 3 stages of network analysis in healthy individuals was the absence of strong correlations between VOCs and plasma parameters. In contrast, numerous correlations were present between spectral indicators and VOCs in patients with ischemic heart disease.

Focusing on inflammatory markers, a moderate negative correlation between CRP and HDL was detected in healthy controls, but not in patients. Conversely, a moderate inverse correlation between IL-6 and total cholesterol was observed in patients.

https://doi.org/10.12997/jla.2025.14.3.350

Additionally, a consistent negative association between HDL and lipid-lowering therapy was present at all time points in the control group—which is expected—while this relationship was weak in the patient group, with no significant differences between groups for this parameter.

The study identified 2-ethyl-2,5-dihydro-4,5-dimethylthiazole, HO_3PS_2, CH_8N_3P, and m/z 49.99501251 as the most important VOCs associated with both the lipid profile and inflammatory biomarkers. However, the biochemical origin of these molecules in exhaled breath remains uncertain and warrants further investigation.

2-Ethyl-2,5-dihydro-4,5-dimethylthiazole is a thiazole derivative, a heterocyclic compound containing sulfur and nitrogen.[29,30] Thiazoles and their derivatives are often studied for their biological activities, including potential roles in metabolism, or as biomarkers. In the context of heart disease, thiazole derivatives are of interest regarding their potential effects on cellular metabolism, oxidative stress, or inflammation, which are key factors in IHD.[31,32] However, specific studies directly linking this compound to IHD are not readily available in the literature.

The molecular formulas HO_3PS_2 and CH_8N_3P suggest that these compounds may be related to biochemical pathways or metabolic processes that could influence heart health. However, specific connections between these formulas and heart disease are not detailed in the literature.

HO_3PS_2 contains phosphorus and sulfur, which are elements involved in various biochemical processes.[33] Phosphorothioates are often used in biochemistry and molecular biology, such as in oligonucleotide synthesis.[34,35] In heart disease, phosphorus-containing compounds are critical for energy metabolism (e.g., ATP), and disruptions in phosphorus metabolism can contribute to cardiovascular dysfunction.[33,36]

CH_8N_3P is a small molecule containing phosphorus and nitrogen. Phosphorus-containing compounds are essential in cellular energy transfer and signaling pathways.[37] In the context of IHD, such compounds might be relevant in studies of mitochondrial dysfunction or energy metabolism, which are often impaired in ischemic conditions.[38,39]

The high m/z value of 49.99501251 may correspond to a large biomolecule, such as a protein, peptide, or complex metabolite. In mass spectrometry, such peaks can represent either biomarkers or degradation products associated with heart disease.[40,41] Proteomic and metabolomic studies in IHD frequently identify dysregulated proteins and metabolites that may serve as diagnostic or prognostic markers.[42,43]

Future research should focus on validating the specificity of these identified VOCs in larger, independent cohorts. It will also be important to explore the biochemical pathways connecting thiazole derivatives and phosphorus-containing compounds to the progression of IHD, and to investigate how lipid-lowering therapies may alter VOC profiles to further refine therapeutic monitoring strategies.

This study demonstrates complex interactions between lipid profiles, inflammatory markers, and VOCs in patients with ischemic heart disease, with clear distinctions between patients and healthy controls. The findings indicate that 2-ethyl-2,5-dihydro-4,5-dimethylthiazole, HO3PS2, CH8N3P, and m/z 49.99501251 are among the most important VOCs, each showing relationships with both the lipid profile and inflammation biomarkers. Notably, patients with

https://doi.org/10.12997/jla.2025.14.3.350

JLA Journal of Lipid and Atherosclerosis

IHD exhibited numerous correlations between lipid spectrum indicators and VOCs, such as a positive correlation between HDL and m/z 49.995012 (r=0.31), and a negative correlation between total cholesterol and m/z 94.053730 (r=–0.35).

SUPPLEMENTARY MATERIALS

Supplementary Table 1
Selection criteria for the study participants

Supplementary Table 2
The exhaled breath predictors (listed as column factors) correspond to the mass/charge (m/z) ratio, the sign in the predictor names "_" is "."

Supplementary Table 3
The predictors of the exhaled breath (column factors) are the same the mass/charge ratio, the sign in the predictor names "_" is "."

Supplementary Table 4
Correlation test, delta 1 for volatile organic compounds, patients group. In the variable names of the exhaled breath predictors, the underscore "_" represents a decimal point (".")

Supplementary Table 5
Correlation test, delta 1 for volatile organic compounds, control group. In the variable names of the exhaled breath predictors, the underscore "_" represents a decimal point (".")

Supplementary Table 6
Correlation test, delta 3 for volatile organic compounds, for patients group. In the variable names of the exhaled breath predictors, the underscore "_" represents a decimal point (".")

Supplementary Table 7
Correlation test, delta 3 for volatile organic compounds, control group. In the variable names of the exhaled breath predictors, the underscore "_" represents a decimal point (".")

Supplementary Table 8
Correlation test, common volatile organic compounds for delta 1 and delta 3, patients group. In the variable names of the exhaled breath predictors, the underscore "_" represents a decimal point (".")

Supplementary Table 9
Correlation test, common volatile organic compounds for delta 1 and delta 3, control group. The sign in the variable's names of the predictors of the exhaled breath "_" is ".", and they are the same the mass/charge ratio of the found volatile organic compounds

Supplementary Table 10
Annotation of the obtained m/z according to the built machine learning model

https://doi.org/10.12997/jla.2025.14.3.350

REFERENCES

1. Martin SS, Aday AW, Almarzooq ZI, Anderson CAM, Arora P, Avery CL, et al. 2024 Heart disease and stroke statistics: a report of US and global data from the American Heart Association. Circulation 2024;149:e347-e913. PUBMED | CROSSREF
2. Knuuti J, Wijns W, Saraste A, Capodanno D, Barbato E, Funck-Brentano C, et al. 2019 ESC guidelines for the diagnosis and management of chronic coronary syndromes. Eur Heart J 2020;41:407-477. PUBMED | CROSSREF
3. Gulati M, Levy PD, Mukherjee D, Amsterdam E, Bhatt DL, Birtcher KK, et al. 2021 AHA/ACC/ASE/CHEST/SAEM/SCCT/SCMR guideline for the evaluation and diagnosis of chest pain: a report of the American College of Cardiology/American Heart Association Joint Committee on clinical practice guidelines. J Cardiovasc Comput Tomogr 2022;16:54-122. PUBMED | CROSSREF
4. Gulati M, Levy PD, Mukherjee D, Amsterdam E, Bhatt DL, Birtcher KK, et al. 2021 AHA/ACC/ASE/CHEST/SAEM/SCCT/SCMR guideline for the evaluation and diagnosis of chest pain: a report of the American College of Cardiology/American Heart Association Joint Committee on clinical practice guidelines. Circulation 2021;144:e368-e454. PUBMED | CROSSREF
5. Barbarash OL, Karpov YA, Panov AV, Akchurin RS, Alekyan BG, Alekhine MN, et al. Stable ischemic heart disease. Clinical guidelines 2024. Russ J Cardiol 2024;29:6110. CROSSREF
6. Nakano S, Kohsaka S, Chikamori T, Fukushima K, Kobayashi Y, Kozuma K, et al. JCS 2022 guideline focused update on diagnosis and treatment in patients with stable coronary artery disease. Circ J 2022;86:882-915. PUBMED | CROSSREF
7. Marzoog BA. Volatilome: a novel tool for risk scoring in ischemic heart disease. Curr Cardiol Rev 2024;20:e080724231719. PUBMED | CROSSREF
8. Mancini GBJ, Gosselin G, Chow B, Kostuk W, Stone J, Yvorchuk KJ, et al. Canadian Cardiovascular Society guidelines for the diagnosis and management of stable ischemic heart disease. Can J Cardiol 2014;30:837-849. PUBMED | CROSSREF
9. Marzoog BA. Volatilome is inflammasome- and lipidome-dependent in ischemic heart disease. Curr Cardiol Rev 2024;20:e190724232038. PUBMED | CROSSREF
10. Marzoog B. Breathomics detect the cardiovascular disease: delusion or dilution of the metabolomic signature. Curr Cardiol Rev 2024;20:e020224226647. PUBMED | CROSSREF
11. Marzoog BA, Chomakhidze P, Gognieva DG, Gagarina NV, Kopylov P. Methods enhancing the diagnostic accuracy of the bicycle ergometry in ischemic heart disease. Curr Cardiol Rev. Forthcoming 2024.
12. Marzoog BA, Chomakhidze P, Gognieva D, Parunova AY, Demchuk SN, Silantyev A, et al. Updates in breathomics behavior in ischemic heart disease and heart failure, mass-spectrometry. World J Cardiol 2025;17:102851. PUBMED | CROSSREF
13. Marzoog BA, Kopylov P. Volatilome and machine learning in ischemic heart disease: current challenges and future perspectives. World J Cardiol 2025;17:106593. PUBMED | CROSSREF
14. Dharmawardana N, Woods C, Watson DI, Yazbeck R, Ooi EH. A review of breath analysis techniques in head and neck cancer. Oral Oncol 2020;104:104654. PUBMED | CROSSREF
15. Janssens E, van Meerbeeck JP, Lamote K. Volatile organic compounds in human matrices as lung cancer biomarkers: a systematic review. Crit Rev Oncol Hematol 2020;153:103037. PUBMED | CROSSREF
16. Lombardi M, Segreti A, Miglionico M, Pennazza G, Tocca L, Amendola L, et al. Breath analysis via gas chromatography-mass spectrometry (GC-MS) in chronic coronary syndrome (CCS): a proof-of-concept study. J Clin Med 2024;13:5857. PUBMED | CROSSREF
17. Marzoog BA, Chomakhidze P, Gognieva D, Gagarina NV, Silantyev A, Suvorov A, et al. Machine learning model discriminate ischemic heart disease using breathome analysis. Biomedicines 2024;12:2814. PUBMED | CROSSREF
18. Cockcroft DW, Gault MH. Prediction of creatinine clearance from serum creatinine. Nephron J 1976;16:31-41. PUBMED | CROSSREF
19. Winter MA, Guhr KN, Berg GM. Impact of various body weights and serum creatinine concentrations on the bias and accuracy of the Cockcroft-Gault equation. Pharmacotherapy 2012;32:604-612. PUBMED | CROSSREF
20. Brown DL, Masselink AJ, Lalla CD. Functional range of creatinine clearance for renal drug dosing: a practical solution to the controversy of which weight to use in the Cockcroft-Gault equation. Ann Pharmacother 2013;47:1039-1044. PUBMED | CROSSREF
21. Delgado C, Baweja M, Crews DC, Eneanya ND, Gadegbeku CA, Inker LA, et al. A unifying approach for GFR estimation: recommendations of the NKF-ASN task force on reassessing the inclusion of race in diagnosing kidney disease. Am J Kidney Dis 2022;79:268-288.e1. PUBMED | CROSSREF

22. Horváth I, Barnes PJ, Loukides S, Sterk PJ, Högman M, Olin AC, et al. A European Respiratory Society technical standard: exhaled biomarkers in lung disease. Eur Respir J 2017;49:1600965. PUBMED | CROSSREF
23. SCORE2 working group and ESC cardiovascular risk collaboration. SCORE2 risk prediction algorithms: new models to estimate 10-year risk of cardiovascular disease in Europe. Eur Heart J 2021;42:2439-2454. PUBMED | CROSSREF
24. Dorresteijn JAN, Visseren FLJ, Wassink AMJ, Gondrie MJA, Steyerberg EW, Ridker PM, et al. Development and validation of a prediction rule for recurrent vascular events based on a cohort study of patients with arterial disease: the SMART risk score. Heart 2013;99:866-872. PUBMED | CROSSREF
25. Hastie T, Tibshirani R, Friedman JH. The elements of statistical learning: data mining, inference, and prediction. Springer; 2009.
26. Wishart DS, Guo A, Oler E, Wang F, Anjum A, Peters H, et al. HMDB 5.0: the human metabolome database for 2022. Nucleic Acids Res 2022;50:D622-D631. PUBMED | CROSSREF
27. Nagasawa N, Nakamura S, Ota H, Ogawa R, Nakashima H, Hatori N, et al. Relationship between microvascular status and diagnostic performance of stress dynamic CT perfusion imaging. Eur Radiol 2024;35:2855-2865. PUBMED | CROSSREF
28. Michallek F, Nakamura S, Ota H, Ogawa R, Shizuka T, Nakashima H, et al. Fractal analysis of 4D dynamic myocardial stress-CT perfusion imaging differentiates micro- and macrovascular ischemia in a multi-center proof-of-concept study. Sci Rep 2022;12:5085. PUBMED | CROSSREF
29. Mandadapu SR, Weerawarna PM, Prior AM, Uy RAZ, Aravapalli S, Alliston KR, et al. Macrocyclic inhibitors of 3C and 3C-like proteases of picornavirus, norovirus, and coronavirus. Bioorg Med Chem Lett 2013;23:3709-3712. PUBMED | CROSSREF
30. Chhabria MT, Patel S, Modi P, Brahmkshatriya PS. Thiazole: a review on chemistry, synthesis and therapeutic importance of its derivatives. Curr Top Med Chem 2016;16:2841-2862. PUBMED | CROSSREF
31. Libby P, Ridker PM, Hansson GK; Leducq Transatlantic Network on Atherothrombosis. Inflammation in atherosclerosis: from pathophysiology to practice. J Am Coll Cardiol 2009;54:2129-2138. PUBMED | CROSSREF
32. Meurillon M, Marton Z, Hospital A, Jordheim LP, Béjaud J, Lionne C, et al. Structure-activity relationships of β-hydroxyphosphonate nucleoside analogues as cytosolic 5′-nucleotidase II potential inhibitors: synthesis, in vitro evaluation and molecular modeling studies. Eur J Med Chem 2014;77:18-37. PUBMED | CROSSREF
33. Tonelli M, Sacks F, Pfeffer M, Gao Z, Curhan G; Cholesterol And Recurrent Events Trial Investigators. Relation between serum phosphate level and cardiovascular event rate in people with coronary disease. Circulation 2005;112:2627-2633. PUBMED | CROSSREF
34. Evans K, Nasim Z, Brown J, Clapp E, Amin A, Yang B, et al. Inhibition of SNAT2 by metabolic acidosis enhances proteolysis in skeletal muscle. J Am Soc Nephrol 2008;19:2119-2129. PUBMED | CROSSREF
35. Eckstein F. Phosphorothioates, essential components of therapeutic oligonucleotides. Nucleic Acid Ther 2014;24:374-387. PUBMED | CROSSREF
36. Neubauer S. The failing heart--an engine out of fuel. N Engl J Med 2007;356:1140-1151. PUBMED | CROSSREF
37. Ingwall JS. Energy metabolism in heart failure and remodelling. Cardiovasc Res 2009;81:412-419. PUBMED | CROSSREF
38. Lesnefsky EJ, Chen Q, Hoppel CL. Mitochondrial metabolism in aging heart. Circ Res 2016;118:1593-1611. PUBMED | CROSSREF
39. Smith RAJ, Murphy MP. Mitochondria-targeted antioxidants as therapies. Discov Med 2011;11:106-114. PUBMED
40. Gerszten RE, Wang TJ. The search for new cardiovascular biomarkers. Nature 2008;451:949-952. PUBMED | CROSSREF
41. Dettmer K, Aronov PA, Hammock BD. Mass spectrometry-based metabolomics. Mass Spectrom Rev 2007;26:51-78. PUBMED | CROSSREF
42. McGarrah RW, Crown SB, Zhang GF, Shah SH, Newgard CB. Cardiovascular metabolomics. Circ Res 2018;122:1238-1258. PUBMED | CROSSREF
43. Rosendorff C, Lackland DT, Allison M, Aronow WS, Black HR, Blumenthal RS, et al. Treatment of hypertension in patients with coronary artery disease: a scientific statement from the American Heart Association, American College of Cardiology, and American Society of Hypertension. J Am Coll Cardiol 2015;65:1998-2038. PUBMED | CROSSREF